

## Simultaneous inversion of AEM data for 3D conductivity and chargeability: Case study of TargetEM data, Canada

### Introduction

A new active time domain airborne EM system, Target EM, has been demonstrated for targeting discrete conductors and contrasting stratigraphy. The system has been developed with high-resolution quantitative inversion in mind with low noise, high power, and a small transmitter-receiver offset. A new inversion methodology that considers both EM induction and induced polarization (IP) effects has been introduced. The end product consists of a three-dimensional (3D) physical parameter model, which includes conductivity, chargeability, time constant, and relaxation coefficients. All time channels and components from the AEM system are included in the 3D modeling and inversion. In this paper, we discuss the underlying principles of this methodology and show an example of a high-resolution 3D model that can be obtained from carefully collected and processed airborne EM data and an advanced 3D inversion.

### TargetEM System Description

The TargetEM is a new patent pending airborne time domain electromagnetics system. It combines the latest achievements in electronics and sophisticated signal processing techniques to reliably deliver high-resolution geoelectrical data. The system uses full waveform recording at a digitizing rate of 73,728 Hz. The maximum dipole moment is 700,000, NIA, depending on the transmitter loop diameter and number of turns. The loop diameter is typically 21 m to 31 m. The base frequency is 25 or 30 Hz, depending on the local powerline frequency. The system collects inline, crossline, and vertical db/dt data (processed B-field data is also delivered). The time range is from 70 us to 14 ms after turn off depending on the base frequency and transmitter pulse width. It has an in-loop geometry. Both VLF and AFMAG data are collected along with the time-domain EM data.

### Theory and Methods

For both 1D and 3D inversions, modeling is conducted in the frequency domain and then predicted data and sensitivities are transformed into the time domain. This allows induced polarization (IP) to be easily included in the modeling and inversion. We use the simplified GEMTIP model (Zhdanov, 2008) to parameterize the induced polarization effects:

$$\sigma(\omega) = \sigma \left( 1 + \eta \left( 1 - \frac{1}{1 + (i\omega\tau)^C} \right) \right)$$

where  $\sigma$  is the DC conductivity (S/m);  $\omega$  is the angular frequency (rad/sec),  $\tau$  is the time constant;  $\eta$  is the intrinsic chargeability, and  $C$  is the relaxation parameter. The dimensionless intrinsic chargeability,  $\eta$ , characterizes the intensity of the IP effect.

The inversion is run using a stabilized reweighted conjugate gradient scheme for conductivity, chargeability, time constant, and relaxation parameter, as outlined by Cox et al. (2023). For both the 1D and 3D inversions, the earth is discretized into voxels, and the electrical parameters are recovered for each voxel during inversion. The sensitivities for conductivity in the 1D inversion are computed by perturbation, and for the 3D inversion are computed by reciprocity. The sensitivities for the IP parameters are computed using the chain rule based on analytic derivatives, so almost no additional computation time is required to fully include induced polarization in the modeling.

The interpretation workflow begins with gridding apparent chargeability, conductivity, time constant, and relaxation coefficient into a 3D grid. This is used as a starting model for the 1D inversion of the vertical component of the AEM data. The inline (X) component cannot be used with most modern systems because, with a small (or zero) transmitter-receiver offset, the sensitivity of the inline component to a layered earth is very small (or zero). The 1D inversion results are then smoothed by convolution with a boxcar function, which is laterally the size of the instrument's sensitivity footprint.

The rationale for this is that 1D inversion produces reasonable results in locations where the earth is laterally invariant within the footprint of the instrument. In this case, lateral smoothing will not change the model appreciably. In areas where later variations are strong, the 1D inversion will contain artifacts and generally incorrect geometry and conductivity contrasts, which are too weak. In this case, the smoothing of the 1D model will create a smooth background conductivity and starting model for the 3D inversion.

The 3D modeling and sensitivity calculation is done with a hybrid finite difference (FD) and integral equation (IE) scheme. The FD is used to calculate the electric field within the anomalous domain. It follows the basic ideas of Newman and Alumbaugh (1995) and uses a modified version of Yoon et al. (2016). The method solves Maxwell's equations in the frequency domain based on a finite-difference scheme on a staggered grid and uses the anomalous field formulation with the total field being decomposed into background,  $\mathbf{E}^b$ , and anomalous,  $\mathbf{E}^a$ , fields. The calculation of the anomalous field with an equivalent source makes it possible to avoid the discretization problems associated with discrete sources. It is also simplified using different sources, such as a loop versus a vertical dipole or an arbitrarily oriented dipole. This approach has been widely used in the EM modeling literature, whether with FD, finite-volume, finite-element, or IE methods (e.g., Zhdanov, 2002). We use the Paradiso direct solver so that the many sources and adjoint sources can be solved nearly simultaneously.

To speed up and stabilize the computations, we then use an IE approach to calculate the electric and magnetic fields at the receivers based on the anomalous electric field computed by the FD method. The anomalous electric and magnetic fields at the receiver position,  $\mathbf{r}_j, j = 1, 2, \dots, L$ , can be expressed as an integral over the excess currents in the inhomogeneous domain  $D$ :

$$\mathbf{H}^a(\mathbf{r}_j) = \iiint_D \mathbf{G}_H(\mathbf{r}_j|\mathbf{r}) \Delta\sigma(\mathbf{r}) \cdot \mathbf{E}^T(\mathbf{r}) dV$$

where  $\mathbf{G}_H(\mathbf{r}_j|\mathbf{r})$  is the magnetic Green's tensors defined for an unbounded conductive medium with the normal (horizontally layered) anisotropic conductivity;  $\mathbf{E}^T(\mathbf{r})$  is the total electric field at the point  $\mathbf{r}$  inside the domain, and  $\mathbf{H}^a(\mathbf{r}_j)$  is the anomalous (scattered) magnetic field at receiver  $j$ .

In summary, a multi-step workflow for the 3D inversion of airborne data consists of the following steps:

1. Determining a best-fit polarizable half-space for each transmitter-receiver pair, including conductivity, changeability, time constant, and relaxation coefficient.
2. Gridding the best-fit half-spaces into a 3D voxel model.
3. This model is used as a starting point for initial inversion based on a one-dimensional (1D) approximation to compute data and sensitivities.
4. Smoothing the 1D inversion results.
5. The smoothed 1D inversion results are used as a starting model for full 3D inversion.

## Field Data Example

### *Geology*

The study area is located in the Porcupine Mining District, around 40 km North of Timmins, Northern Ontario. The district is under gold and nickel prospecting with historic geophysical ground and airborne surveys (Kaminski et al., 2011). The property lies in the Abitibi Terrain, eastern part of Superior Province, and is underlain by mafic and ultramafic rocks as well as intermediate metavolcanics. These early Precambrian units have been intruded by several metamorphosed mafic and ultramafic bodies. The area is extensively covered by Quaternary glacial sediments. The overburden thickness may reach 30-50 meters.

### *Survey*

The TargetEM survey was flown along test lines 1060 and 1140 in this area. The mean flight height was 53 m. Vertical (Z) component db/dt data were processed to time channels from 41  $\mu$ s to 8247 ms,

and the inline (X) component data from 514  $\mu$ s to 8247 ms. All time channels and components were used in the 3D inversion, and all time channels from the vertical component were used in the 1D inversion.

*Inversion Parameters*

A starting model was built by finding a best-fit conductive half-space for each transmitter-receiver pair and gridding this into a 3D model. The chargeability was set to 50 mV/V, time constant to  $1e-3$  s, and C to 1 (dimensionless). The data weights for inversion are based on a two-part model: an absolute error plus a relative error. The percent and absolute errors are combined into a total error by the following equation:

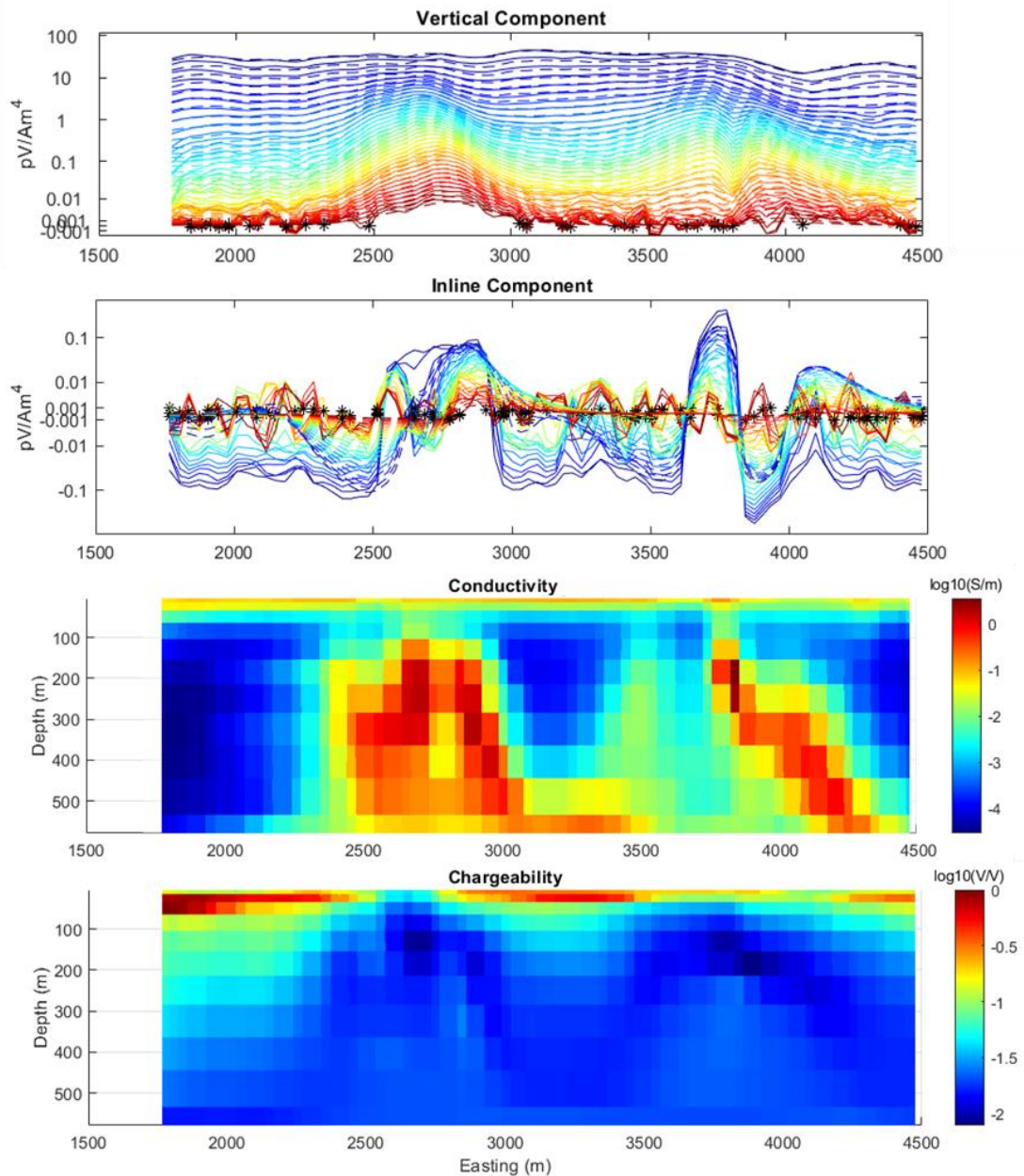


**Figure 1.** The top panel shows observed (-) and predicted (:) data from the vertical  $db/dt$  component. The second pane presents the inline component. The third pane shows the conductivity in the vertical cross section under L1060 extracted from the 3D inversion results, and the last panel shows the chargeability from the 3D inversion results under L1060.

$$e^t = |d_o| * \frac{e^p}{100} + e^a.$$

Absolute error floors were set at 0.003 pV/Am<sup>4</sup> for the vertical component and 0.01 pV/Am<sup>4</sup> for the inline component (3D inversion only), and the percent error was set to 10% for both components. The conductivity and chargeability models derived from the 1D inversion are used as the starting models for 3D inversion.

### Results

Figure 1 shows the vertical sections of 3D inversion results. About 30 m of moderately (~30 Ohm-m) conductive overburden is seen in the 3D model, which is retained from the 1D inversion results. The resolution of the anomalies is dramatically improved from the 1D model, with the contrast increasing and the geometry being corrected. The model fits both the X and the Z component data with the three-dimensionality and induced polarization considered. It is geologically reasonable and fits the observed data, which is what is required from an inversion algorithm.

### Conclusions

The new Target EM system has been shown to collect high-quality multicomponent db/dt data from less than 40 μs to 8 ms. The developed method for 3D inversion of the airborne EM data considers both the EM induction and IP effects simultaneously, so comprehensive quantitative interpretation can be applied to the data for a full physics and dimensional inversion. We apply a robust methodology that builds the 3D model starting from a set of 1D inversions to QC the data. The results of 1D inversions are used to develop an initial approximate model for 3D inversion and provide background conductivities for 3D modeling. The final 3D inversion for conductivity, chargeability, and other IP parameters uses all components, time channels, the dimensionality of the problem, and full physics to arrive at a model that fits the observed data to the noise level in the survey and is geologically reasonable.

### Acknowledgments

The authors thank TechnoImaging, LLC, and Expert Geophysics, LTD, for supporting this work and for permission to publish.

### References

- Cox, L. H., Zhdanov, M. S., Pitcher, D. H., & Niemi, J. [2023]. Three-Dimensional Inversion of Induced Polarization Effects in Airborne Time Domain Electromagnetic Data Using the GEMTIP Model. *Minerals*, 13(6), 779.
- Kaminski, V., Prikhodko, A., Oldenburg, D. [2011]. Using ERA low frequency E-field profiling and UBC 3D frequency-domain inversion to delineate and discover a mineralized zone in Porcupine district, Ontario, Canada. SEG Tech. Program Expanded Abstract.
- Newman, G. A., & Alumbaugh, D. L. [1995]. Frequency-domain modelling of airborne electromagnetic responses using staggered finite differences. *Geophysical Prospecting*, 43(8), 1021-1042.
- Yoon, D., Zhdanov, M. S., Mattsson, J., Cai, H., & Gribenko, A. [2016]. A hybrid finite-difference and integral-equation method for modelling and inversion of marine controlled-source electromagnetic data. *Geophysics*, 81(5), E323-E336.
- Zhdanov, M. S. [2002]. Geophysical inverse theory and regularization problems (Vol. 36). Elsevier.
- Zhdanov, M. S. [2008]. Generalized effective-medium theory of induced polarization. *Geophysics*, 73(5), F197-F211.